Electronic Supplementary Material (ESI) for CrystEngComm

Supplementary Information

Practical microwave-induced hydrothermal synthesis of rectangular-prism-like $CaTiO_3$

L.M. Lozano Sánchez[a], *Soo-Wohn Lee*,[b] *Tohoru Sekino*[c] *and V. Rodríguez-González**[a]

* To whom correspondence should be addressed

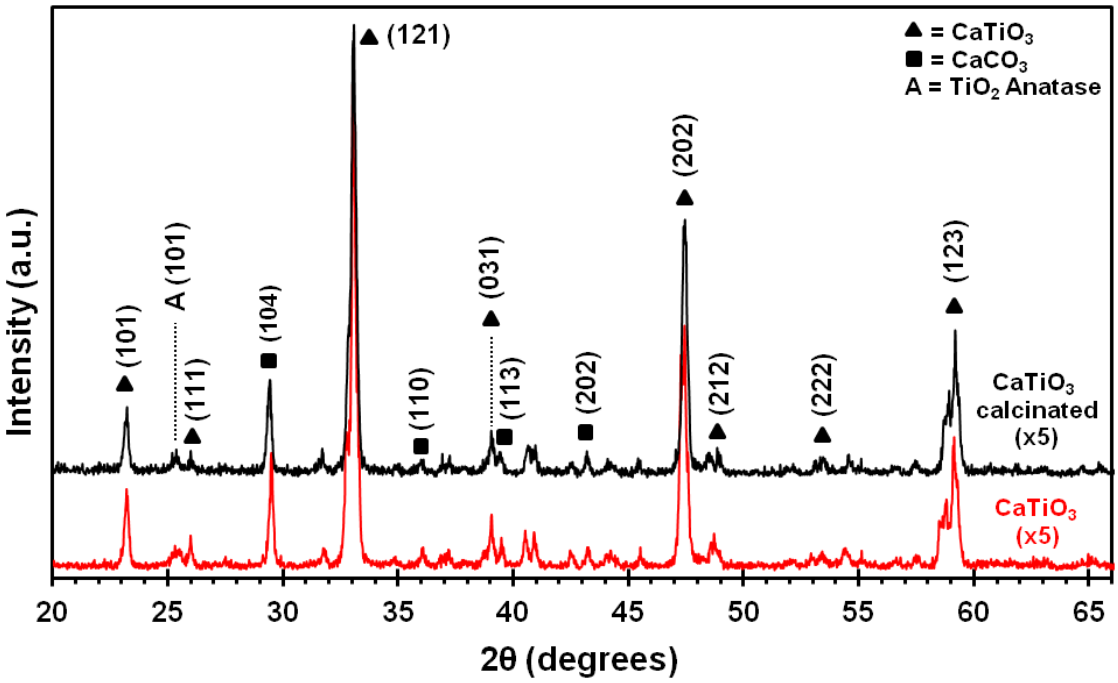

Figure S1. XRD patterns for $CaTiO_3$ cuboid samples and $CaTiO_3$ annealed at 450°C for 4 hr. It can be inferred that cuboids are thermally stable and that no further crystallinity is achieved with the thermal treatment.

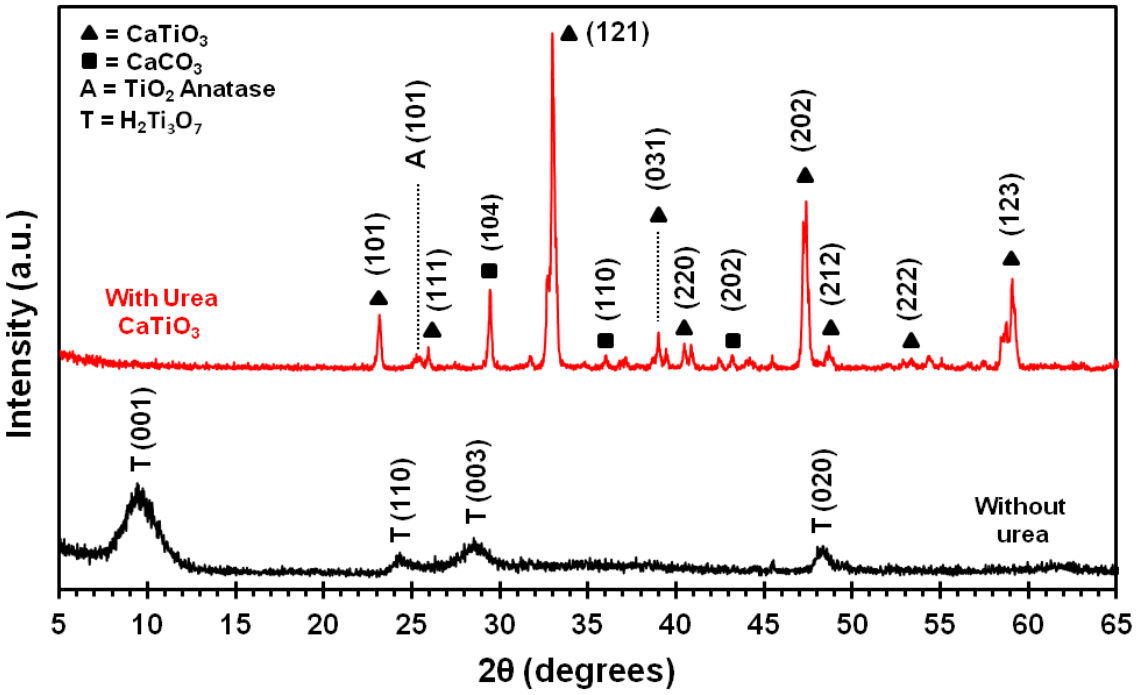

Figure S2. Comparative XRD patterns of samples taken under the same conditions in the microwave-assisted hydrothermal process, obtained to analyze the effect of the urea therein. It can be seen that the reaction that did not contain urea (in black above) resulted in the formation of $H_2Ti_3O_7$ nanotubes and, as mentioned in the text, the use of urea results in the synthesis of cuboid-like particles of $CaTiO_3$.

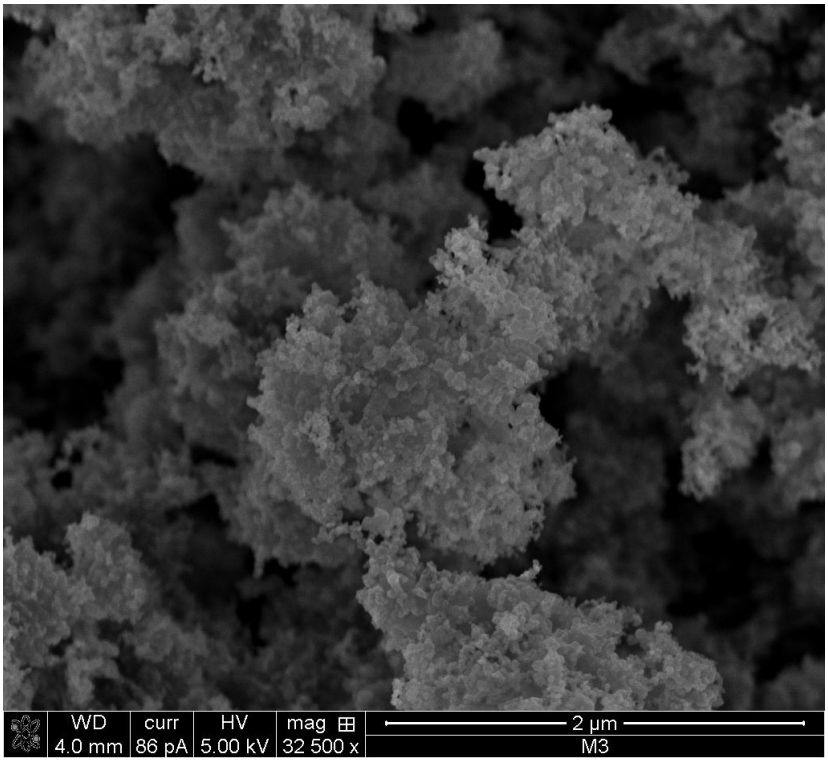

Figure S3. SEM image of bulk TiO_2 P25, used as a precursor in the microwave-assisted hydrothermal synthesis of $CaTiO_3$. It can be inferred that the method proposed in this work achieves a complete transformation of the particles into a homogeneous cuboid morphology.

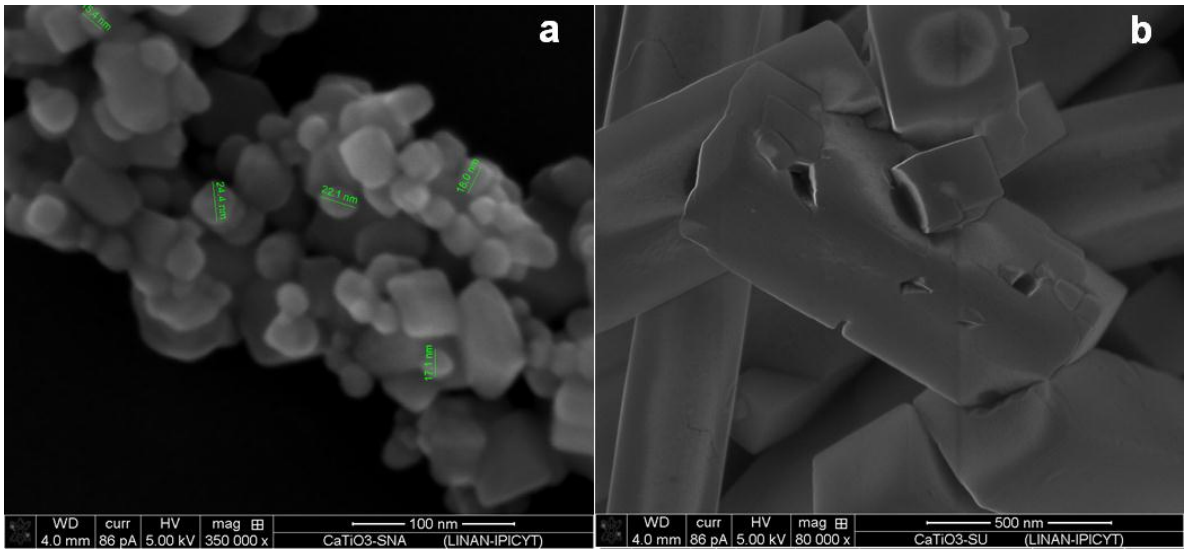

Figure S4. SEM image of $CaTiO_3$ samples synthesized a) without using NaOH, and b) without using urea.

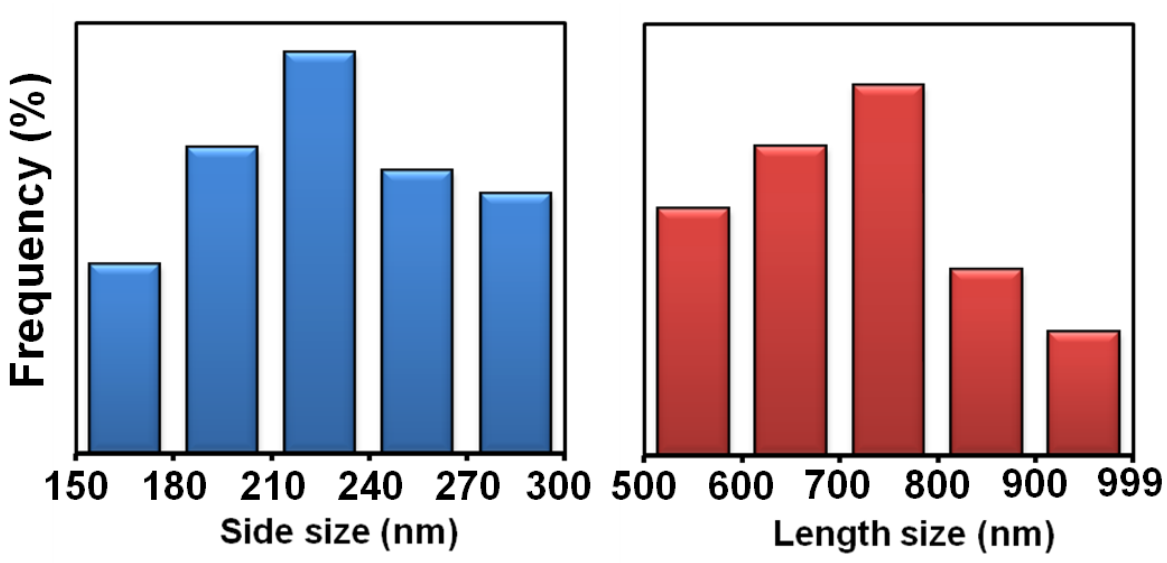

Figure S5. Histograms of dimensional distribution of $CaTiO_3$ particles, where the average dimension is 225 nm x 715 nm.

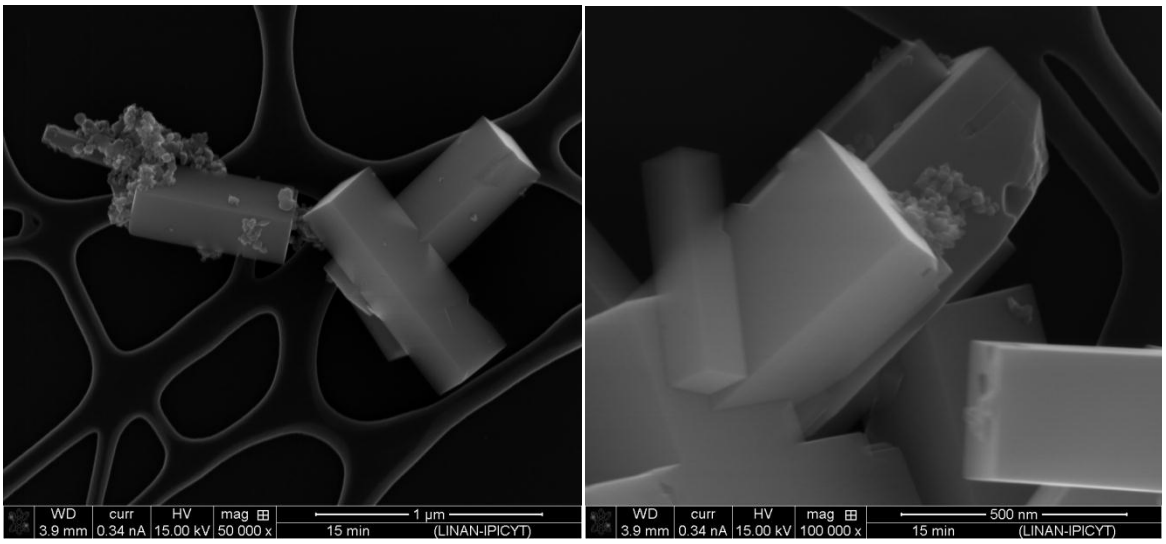

Figure S6. SEM images of $CaTiO_3$ after 15 minutes of reaction in the microwave reactor. Bulk particles are still present, and $CaTiO_3$ cuboids are not completely well-formed, since some significant superficial defects are observed within the particles.

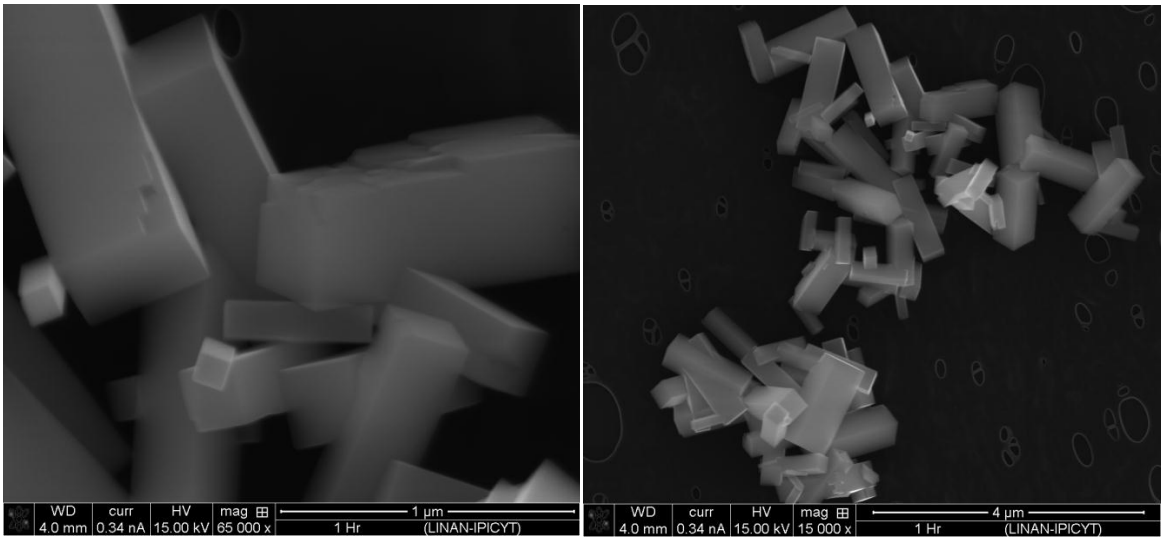

Figure S7. SEM images of $CaTiO_3$ after 1 hour of reaction in the microwave reactor. Even after this longer reaction time, defects are still present on the surface of the cuboids. The size distribution is significantly variable.

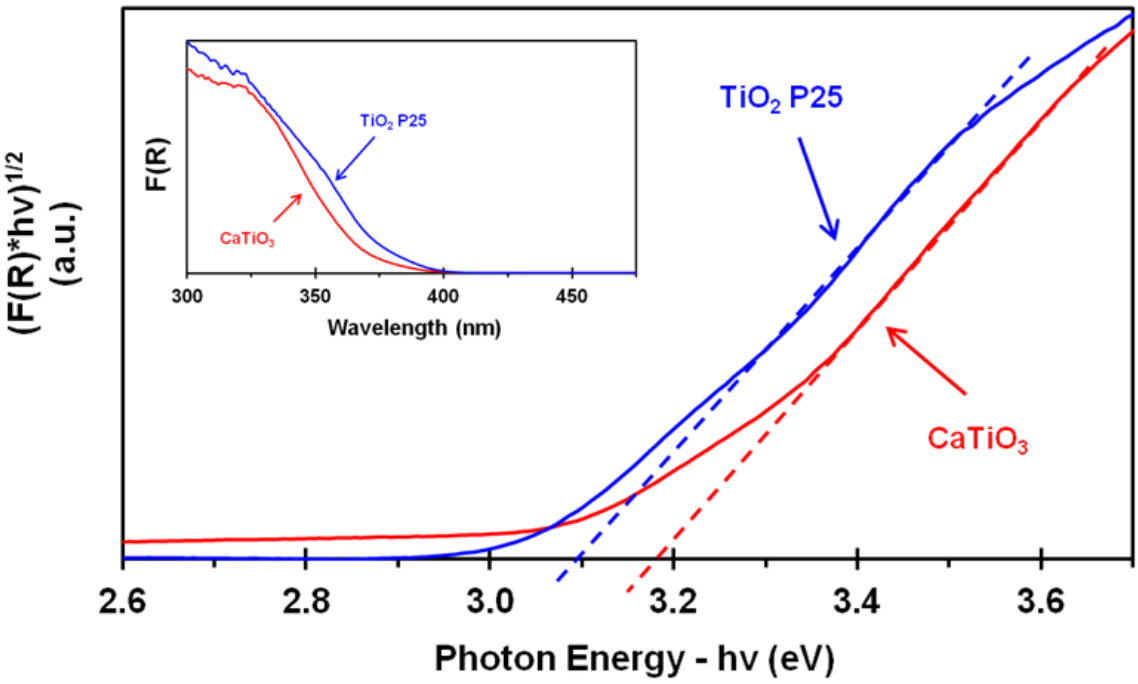

Figure S8. UV-Vis spectra using the Tauc plot model to obtain the band gap energy (E_g) for TiO_2 P25 and perovskite $CaTiO_3$. An increase in the value of the forbidden energy band of the $CaTiO_3$ sample compared to that of the TiO_2 P25 is indicated by the intersection of the dashed line with the blue and red curves.

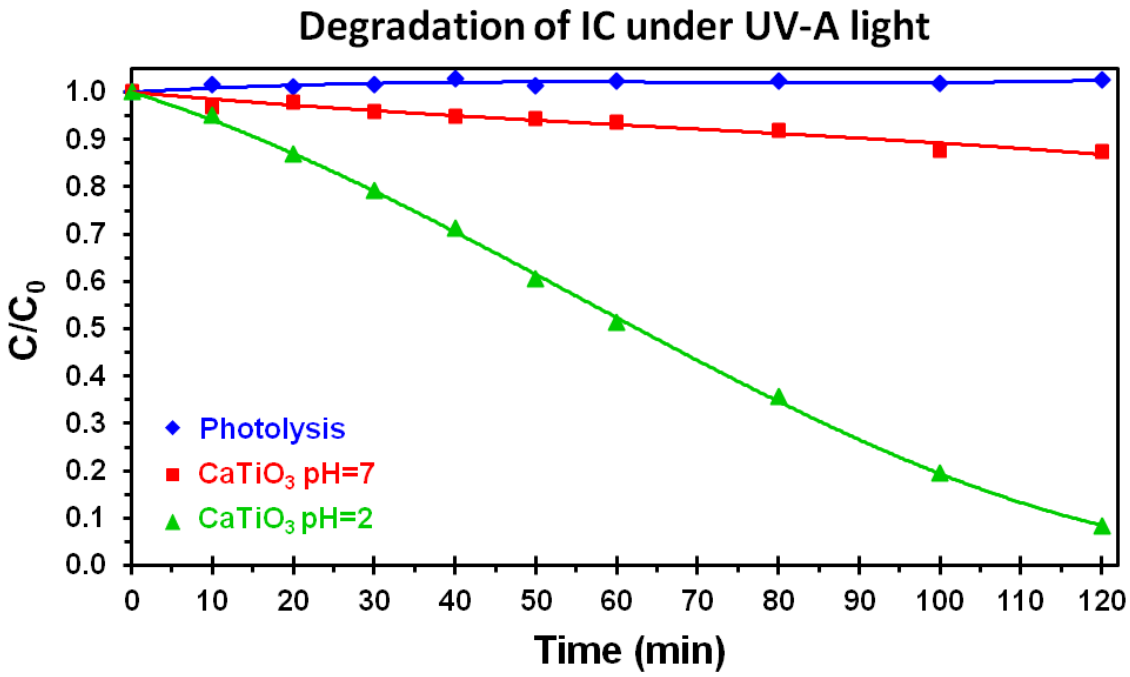

Figure S9. The evaluation of the photocatalytic activity of $CaTiO_3$ sample through the degradation of indigo carmine dye (IC) was performed in a photocatalytic reactor comprising a 20 W lamp of UV-A light irradiation, and a glass reactor of 125 mL capacity placed on a grill with magnetic stirring. 100 mL of IC solution (30 ppm) were placed in the reactor (Pyrex flat Crystallizing Dish), and 100 mg of photocatalyst were then added. The suspension was stirred at 300 rpm. The experiments were performed at room temperature for 120 min (2 hours), and aliquots of 1 mL were collected immediately after each of the 10-minutes of irradiation intervals and analyzed with an UV-Vis spectrophotometer using a 1 mL-capacity quartz cell. The decrease in the concentration of indigo carmine was observed from the characteristic absorption at λ=610 nm. In order to analyze the pH effect of the solution in the degradation of IC, H_2SO_4 was used to perform experiments at acid pH values.

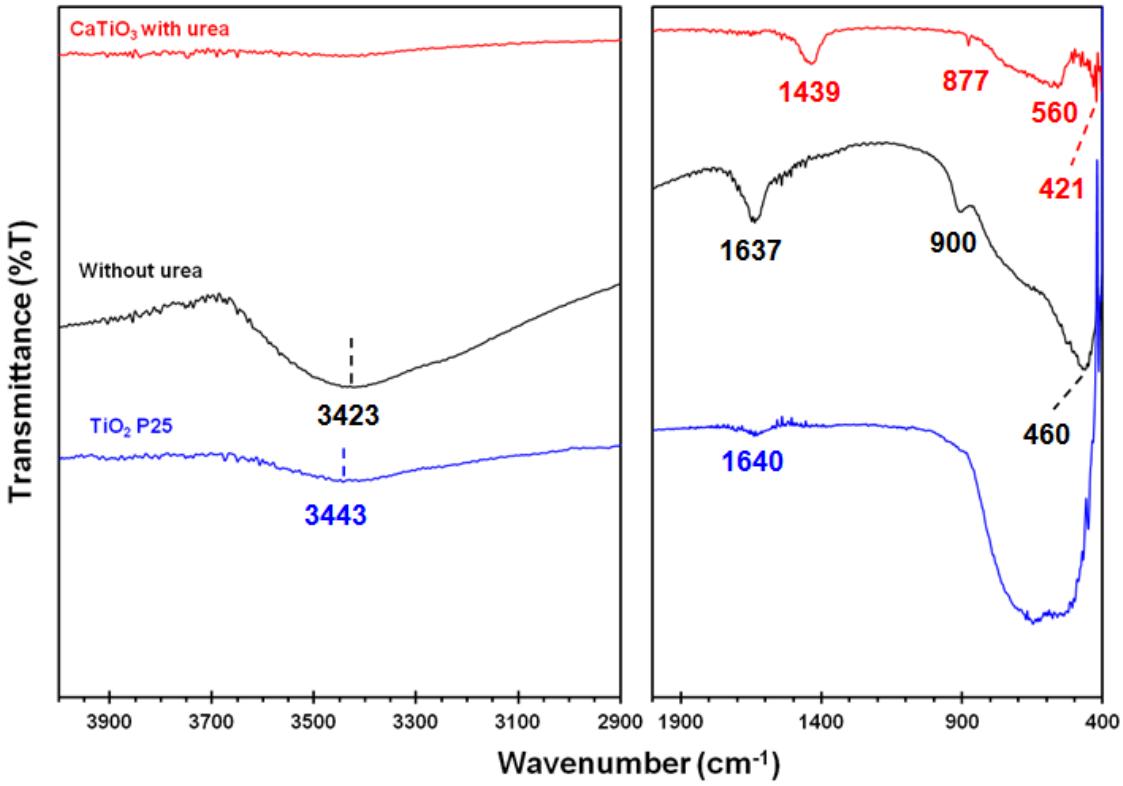

Figure S10. FTIR spectra of (a) perovskite $CaTiO_3$ synthesized by a microwave-assisted hydtrothermal process using urea, for particles with prism-like morphology, and (b) without using urea corresponding to the nanotubes, presented for comparison to show an effect of urea in the process, (c) FTIR spectrum of TiO_2 P25 used as precursor for the reaction. Infrared (IR) spectra were recorded in transmittance mode on a JASCO FTIR-460 plus spectrophotometer. The samples were diluted (10% w/w) in dry KBr and scanned over a frequency range of 400–4000 cm^{-1} at room temperature.

In order to further confirm the bonding structure of the calcium titanate cuboids, an FTIR spectrum was recorded Fig. S6 shows the FTIR spectrum at 400–4000 cm^{-1} of the calcium titanate. The broad band at 2900–3700 cm^{-1} with the transmission peak of 3423 cm^{-1} is the characteristic stretching vibration of hydroxylate (-OH) attributable to water and the bending band is observed at 1650 cm^{-1}. The transmission peak located at 877 cm^{-1} is related to a symmetric stretching vibration along Ca–O–Ca bonds. The transmission band at 1439 cm^{-1} is assigned to the asymmetrical stretching vibration of the hydroxylate (OH–Ca). The transmisson band peak at 560 cm^{-1} is associated with the vibration of the Ca–O bonds of the calcium titanate cuboids.[2] A broad and strong band, characteristic of alkaline titanates, appears at 460 cm^{-1}. The transmission band at 421 cm^{-1} is assigned to the asymmetrical stretching vibration of the Ti-O (from TiO_3^{2-} groups)[3]

1 S. Beg, S. Haneef, and N. A. S. Al-Areqi, *Ioncs.*, 2010, **16**, 239.
2 J. Urban, W. S. Yun, Q. Gu and H. Park, *CrystEngComm. Soc.*, 2012, **14**, 4262.
3 C. Peng, Z. Hou, C. Zhang, G. Li, H. Lian, Z. Cheng and J. Lin, *Opt. Express.*, 2010, **18**, 7543.

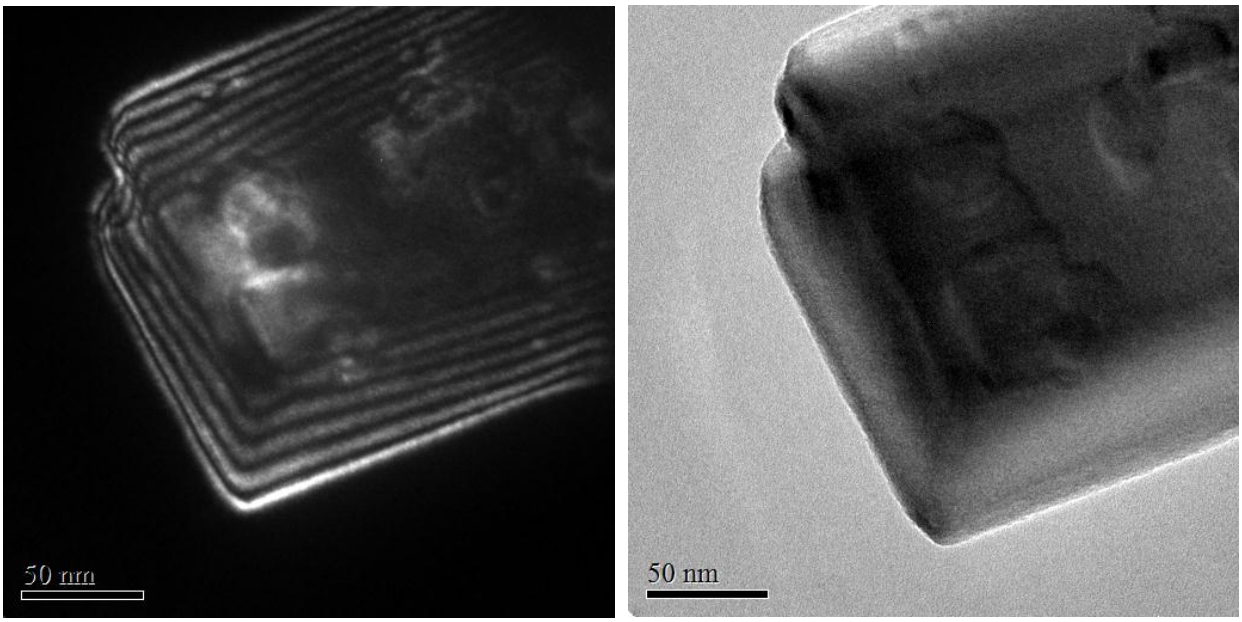

Figure S11. TEM observations in weak-beam dark-field imaging. The layers appear as so called nanosheets. Also, a TEM image of the same particle in bright field is included that confirms the layered structure.